Jenkins, P. G. (2016) Understanding physical changes and strength loss of E-glass fibres following exposure to elevated temperatures. Materials Science and Technology. ISSN 0267-0836 , http://dx.doi.org/10.1080/02670836.2016.1180743

This version is available at https://strathprints.strath.ac.uk/56333/

Understanding strength loss of E-glass fibres following exposure to elevated temperatures

Abstract

The strength loss of glass fibres (GF) following exposure to elevated temperatures is a long-established phenomenon, yet the mechanism or mechanisms responsible for the strength decrease are not fully understood, aside from acknowledgement that surface flaws must become more severe by some means. As disposal of GF based composite materials by landfill has become untenable in many regions, interest in composite recyclability has increased. Separation of GFs from thermosetting polymers generally requires the use of high temperatures, which produces very weak fibres with minimal commercial value. In this context an understanding of the strength loss mechanisms is of importance in terms of efforts to mitigate fibre damage or to recover the strength of previously heated fibres. In addition to fibre strength loss, numerous other physical and chemical changes to heat treated (HT) or recycled GF have been described in the literature.

Peter G. Jenkins, Department of Mechanical & Aerospace Engineering, University of Strathclyde, 75 Montrose Street, Glasgow G1 1XJ, UK

e-mail: peter.jenkins@strath.ac.uk

1. Overview

The review presented examines the current understanding of both physical changes and strength loss of glass fibres caused by exposure to elevated temperatures, with particular focus on E-glass. This discussion, specifically, is addressed in section 4. In the preceding sections, a summary on the nature of E-glass is provided, followed by a brief discussion of the strength of glass fibre and its measurement. Readers knowledgeable in the subject may be familiar with the aspects of E-glass that are summarised; if not these sections serve as an extensive introduction to some material characteristics that are specific to E-glass and to the overall physical and chemical nature of the material. Some of these characteristics are of

particular interest because of the changes which occur in them due to exposure to elevated temperature.

2. Glass fibre

2.1 E-glass: an introduction to recyclability

Glass fibre has been used as a polymer composite reinforcement material for decades since it was first commercially produced by Owens-Corning in the 1930s and is nowadays crucial to the composites industry. It constitutes 90 % of the reinforcement fibre used worldwide and global production of the most common type E-glass is of the order of approximately 7 million metric tons annually [1]. Glass fibre (GF) is a desirable material due to its high specific strength and stiffness, its hardness and resistance to chemical and biological action, in addition to other generally desirable properties such as transparency and thermal and sound insulation. In addition, GFs in both continuous and short fibre form possess a desirable balance of price and processability; they are therefore used widely as fibre reinforcement in a variety of thermoplastic and thermosetting plastic matrix materials.

A significant drawback of thermoset (e.g. epoxy or polyester) based composites (GRP) is their relatively poor recyclability, for example in comparison with lightweight metal alloys or other materials which can be recycled and reformed with relative ease. Separation of the reinforcement fibre from matrix is generally necessary; this requires the application of elevated temperature, and in some cases also the addition of solvents or elevated pressures. Of the available techniques, thermal recycling methods are probably the most technologically advanced [2–4]. Furthermore, these methods theoretically allow for the collection of the fibre fraction following removal of the matrix: this fraction has a large embodied energy due to the high processing temperatures in GF production and may be considered the most valuable fraction in GRP [4]. While thermal recycling methods may allow the recovery of fibre from GRP, the strength (and therefore value) of the recovered fibres is very poor due to exposure to the elevated temperatures; a strength loss of up to 80 – 90 % is commonplace [5–9]. Potential processes to regenerate the strength of thermally recycled GF are a current research topic of interest [10]; understanding the underlying mechanism(s) responsible for the original strength loss is an important part of this work. This paper reviews the literature related to the topic of GF strength loss caused by heat treatment and recycling processes and the possible underlying phenomena that may be responsible, with particular focus on E-glass due to its place as the most widely used form of glass reinforcement fibre [11].

2.2 Glass fibre formulation

Glass fibres are produced using a large selection of naturally occurring minerals, mixed together in various ratios. Commonly, fibres are formed by pulling through bushings from a melt maintained at elevated temperature, although alternative methods exist [11]. On leaving the bushing fibres are rapidly quenched and attenuated to a diameter of generally no more than 25 μm [12]. Many of these fibre types contain a large weight percentage of pure silica (SiO_2), with the addition of other oxides; the balance between these constituents is altered in order to control the desired properties of the final product. The simplest glass system of all, pure silica fibres are amorphous polymers based on tetragonal SiO_4 groups with a silicon atom at their centre. The silicon atoms form a network by sharing the oxygen atoms at the corners of these tetrahedrons.

Amorphous silica has no true melting point but softens from 1650 °C. To enhance the ease of production of glass fibres numerous other minerals containing non-siliceous species are added to silica sand. Some additives producing oxides in the melt such as Al_2O_3 and B_2O_3 are referred to as network formers as they become incorporated into the silica network, effecting a reduction in processing temperature. Other oxides, known as network modifiers, are created in glass mixtures; examples of these are CaO, Na_2O or K_2O.

The purpose of network modifiers is to balance the charges associated with oxygen ions within the network, due to the incorporation of network formers other than silicon. These modifiers are found in the interstices of the glass network. Some further oxides known as intermediates are also used, MgO and TiO_2 for example, which can act as either network formers or modifiers.

Many different formulations of glass fibre exist, their chemical compositions being tailored towards an array of various practical uses [11, 13]. For example, GF formulations with improved acid/alkali resistance, low dielectric constant or particularly high tensile strength are available.

2.3 E-glass

E-glass is the most widely produced of all the formulations of mechanical reinforcement glass fibres, due to the overall balance of desirable properties that it possesses [11]. Although unsuitable for some specialist applications, it is a suitable general purpose fibre formulation. There are broadly two types of E-glass: the incumbent (Table 1) and more recent boron-free formulation (Table 2). With respect to both of these types of E-glass two formulations, (a) and (b), are presented. In both cases the weight percentages used in

production mixtures are quoted as typical ranges; this is an outcome of global variations that exist in composition of the oxides that are available to manufacturers. In some cases, smaller weight fraction components may be left out altogether.

Table 1: Typical formulations of boron containing E-glass, taken from [13]

Component [X]	Typical composition of E-glass (wt%)								
	SiO_2	Al_2O_3	B_2O_3	CaO	MgO	$Na_2O + K_2O$	TiO_2	Fe_2O_3	F_2
Formulation (a)	52-56	12-16	5-10	16-25	0-6	0-2	…	…	…
Formulation (b)	52-56	12-15	4-6	21-23	0.4-4	0-1	0.2-0.5	0.2-0.4	0.2-0.7

Trends towards E-glass formulations without B_2O_3 or fluorine are a consequence of health concerns surrounding the volatilisation of these materials.

Table 2: Typical formulations of boron-free E-glass, taken from [13]

Component [X]	Typical composition of boron-free E-glass (wt%)								
	SiO_2	Al_2O_3	CaO	MgO	TiO_2	Na_2O	K_2O	Fe_2O_3	F_2
Formulation (a)	59	12.1	22.6	3.4	1.5	0.9	…	0.2	…
Formulation (b)	60.1	13.2	22.1	3	0.5	0.6	0.2	0.2	0.1

Typical production mixtures for boron-free E-glass are shown in Table 2. Compared with the incumbent E-glass, these formulations have a higher SiO_2 content and therefore slightly higher characteristic temperatures, as indicated in Table 3.

Table 3: Characteristic temperatures of incumbent and boron-free E-glass, taken from [13]

	Characteristic temperatures (°C)				
	Log3 forming	Liquidus	Softening	Annealing	Straining
E-glass	1160-1196	1065-1077	830-860	657	616
Boron-free E-glass	1260	1200	916	736	691

2.4 Glass surface

In reviewing glass fibre and its strength it is of the utmost importance to discuss the fibre surface, as this is understood to be directly linked to fracture behaviour [14]. Some research into the surface of E-glass can be found in the literature, but a greater volume exists for pure silica. This is a useful place to initiate the discussion as the complexities introduced by adding or altering even one component in a silica or glass system can significantly alter its state and complicate analysis of the surface [15, 16]. The study of pure silica systems began many decades ago [17] and has continued since [16, 18, 19].

2.4.1 Surface hydroxyl groups

Unless it has been treated under certain specific conditions the surface of silica can be assumed to be covered to some extent with hydroxyl (OH) groups; when these hydroxyls are bonded to a silicon atom they are known as silanols. These silanols exist in one of two states: they are either free (isolated) or they are hydrogen bonded with a neighbouring silanol [17]. The overall coverage of hydroxyl groups on a surface is expressed by the hydroxyl number α_{OH}. This value was calculated for many types of silica with a range of specific surfaces by Zhuravlev [20]; for a fully hydroxylated silica he produced the so-called Kiselev-Zhuravlev constant, $\alpha_{OH} = 4.6$ nm^{-2}. A similar value of between $4.2 - 5.4$ nm^{-2} was also reported by Bakaev and Pantano [19] using a hydrogen/deuterium exchange method. The Kiselev-Zhuravlev is generally accepted: differing values for fully hydroxylated silica have been reported with a range $\alpha_{OH} = 1.3 - 9.8$ nm^{-2} but these can be explained by significant differences in materials and methodology [16, 18].

The silanol coverage on a silica surface has been shown to be variable, depending on the application of heat and/or vacuum treatments. Using samples pre-treated simultaneously under vacuum and at various temperatures Zhuravlev [20] presented extensive data regarding dehydration of physically adsorbed water, the dehydroxylation of surface silanols and the rehydroxylation of treated samples. After treatment below 200 °C physically adsorbed water remained on the silica surface. However, following treatment at 200 °C or above the surface was fully dehydrated. Further heating led to further evolution of water, due to dehydroxylation of the surface. Two regions of dehydroxylation were found, one between approximately 200-450 °C and the second above 450 °C. The lower range was attributed to the removal of hydrogen bonded hydroxyls and it was noted that combined hydroxyl coverage halved by 450 °C. Above 450 °C only free hydroxyls remained; a temperature in excess of 1000 °C was required to fully dehydroxylate the surface.

Although it is more complex than simple silica, the surface of E-glass fibre has been shown using angle-resolved XPS [21] to be populated with silanol groups whose concentration is greater than in the bulk of the fibre. Values for the surface hydroxyl coverage of glass samples, rather than silica, obtained using contact angle measurements have also been published. The hydroxyl number of heat cleaned laboratory glass slides was reported as α_{OH} = 2.5 nm^{-2} [22]. For slides of boron-free E-glass, once again carefully cleaned and fully hydrolysed, a value of approx. α_{OH} = 2.4 nm^{-2} was obtained [23]. In both cases it is clear that hydroxyl coverage is significantly lower than that of the idealised fully hydroxylated silica system.

2.4.2 Surfaces of E-glass systems

Although they are both amorphous materials whose surfaces are populated with hydroxyl groups, E-glass and silica cannot be considered directly analogous, as suggested by the significant difference in hydroxyl number. Differences between the surface hydroxyl coverage of silica and more complex glass systems are perhaps not surprising given the changes to the molecular network caused by the additions of various network formers and modifiers in glasses. It has been shown [15] that the addition of one extra glass forming component to silica can significantly alter the surface state as demonstrated by a change in the interaction with adsorbate molecules; its effect on surface hydroxyl coverage has also been demonstrated [24].

The surface of E-glass has been studied by numerous researchers and in a few studies it has been shown that there are differences between the surface and bulk of glass fibres in terms of composition at an atomic level. Wong [25] used Auger Electron Spectroscopy to compare the elemental compositions of E-glass fibre surfaces with the bulk (obtained by analysis of fracture surfaces). His results suggested that the fibre surface is rich in silicon, a result also reported by Thomason and Dwight [26]. Wong also reported an enrichment of aluminium at the surface, but to a lesser extent compared with silicon. Conversely, the surface of the fibres studied appeared to have significantly lower concentration of calcium and magnesium compared to the fibre bulk. The conclusion of a calcium-depleted surface was also reported by Nichols et al. [27]. Using X-ray Photoelectron Spectroscopy (XPS) they measured the Ca/Si peak ratio and showed that the calcium concentration at the surface was lower than the bulk value. Similar results – of a silicon- and oxygen-rich and calcium-depleted surface – have also been reported by Wang et al. [28] but using thin glass slides of E-glass composition rather than fibres directly. Studies using plate-glass of E-glass composition, rather than fibre, can simplify measurements due to their flat surface although

they cannot be assumed to be analogous to E-glass fibres in their chemical molecular structure [29].

2.5 Interaction with water

2.5.1 Effect on tensile strength of fibres

From the moment they are drawn, the strength of glass fibres begins a downwards trajectory. At the first instant a fibre will be at close to the intrinsic strength (Section 3.1) associated with the formulation it is manufactured from, but exposure to both mechanical and chemical attack causes a decrease in tensile strength over time. The effect of atmospheric moisture on the development of E-glass fibre strength was investigated by Martin et al. [30] using freshly drawn fibres aged in controlled relative humidity. Exposure to moisture caused a decrease in strength with time; the authors postulated that this was related to an increase in the surface area of so-called macropores, which they defined as pores with a radius $r_p > 10$ nm.

Numerous theories have been proposed to explain the mechanism causing strength loss due to water exposure [31–37]. The details are not relevant to the discussion of strength loss of heat treated (HT) and recycled GF (which relates to extrinsic strength only) as these mechanisms apply to decreases from the intrinsic strength of glasses which is initially very high. The differences between these types of strength are discussed in Section 3.1.

2.5.2 Adsorption of water on E-glass

Previous investigations have suggested that the E-glass surface is hydrophilic, possessing adsorbed multi-layers of water that form over time [38–40]. The adsorption of water may also promote an increase in specific surface that is related to increase in roughness or microporosity [39]. Removal of the adsorbed water layers from E-glass fibre has been reported to occur in the temperature range 55- 200 °C [40]: this upper temperature limit agrees with findings for the removal of adsorbed water on silica [20].

2.6 Glass fibre bulk structure

In addition to an understanding of the GF surface, which is critical to the fracture behaviour, it is also important to understand the structure of the fibre bulk. The bulk structure of GF is distinct from massive glass of the same composition due to effects of the fibre drawing process.

2.6.1 Non-equilibrium structure and fictive temperature (T_f)

Glass fibres have what may be termed a non-equilibrium structure due to the very high rate of quenching they experience during manufacture, in addition to significant longitudinal stresses from fibre pulling (discussed in detail in 2.6.3). The very fast quenching results in the 'freezing-in' of a structure, corresponding to that of an equilibrium liquid; the fictive temperature (T_f) describes the temperature of this equilibrium liquid which possesses similar structure to the non-equilibrium GF. Fictive temperatures for GFs such as E-glass tend to be high because of the fast cooling experienced; thicker fibres of similar composition will have a lower T_f. Fictive temperature correlates with GF material properties of more immediate relevance, for example there is an inverse relationship between T_f and density [41]. This work, however, also demonstrated the complexities of inter-relationships of fibre drawing parameters: for example, at constant fibre diameter an increase in T_f produced an increase in GF density rather than the expected decrease, due to the effect of fibre drawing stresses.

Some data regarding the Young's modulus and the hardness of E-glass fibres were presented by Lonnroth et al. [42]. Their data suggested a slight decrease in both modulus and hardness with decreasing fibre diameter; related to the higher fictive temperature and correspondingly more 'open' fibre structure. Comparability of these results with those of other researchers may, however, be slightly problematic as the wool fibres were produced by cascade spinning process [43] rather than by drawing from a bushing during which a longitudinal stress is applied throughout. The natural range of fibre diameters that may be obtained from cascade spinning differs significantly from fibre drawing, where a desired change in diameter necessitates changes in drawing speed (which correspondingly will affect drawing stress) [44].

2.6.2 Bulk structural orientation

Glass fibre demonstrates significantly superior tensile strength compared to massive glass of similar composition; it has been theorised that this might be explained in part by an orientation of structure whereby bonds within the material are formed with some preferential direction. In the case of glass fibre, if orientation were present, the assumption was that the 'strong' bonds would be along the longitudinal direction of the fibre. This differs from other orientations, for example the drawing out of any heterogeneities persisting in the melt [45]. Although evidence of orientation of structure has been presented for other glass systems [46–48] it has not been evidenced for E-glass and it is a matter of agreement that its structure is isotropic [45, 49, 50].

2.6.3 Anisotropy orientation and birefringence

Although it has been argued convincingly in the literature that the structure of E-glass fibre is isotropic there is, however, a separate discussion regarding a different type of orientation in glass fibre. This may be referred to as axial or optical anisotropy and it is quantified by measuring birefringence. If a material is birefringent its refractive index is different depending on the polarisation or direction of light passing through it. This property is imparted to glass fibres due to straining during the fibre drawing process [51]. Stockhorst and Brückner [41] measured birefringence (Δn) of E-glass fibre bundles drawn from a constant melt, but varied production parameters such as nozzle temperature, drawing speed and drawing force, as shown in Figure 1. The birefringence of fibres was shown to increase with increasing drawing speed and drawing force. For a constant birefringence, fibres drawn from a hotter nozzle required a smaller stress but, conversely, a greater drawing speed. From a structural point of view, the authors suggested that the glass melt structure is more "open" after flow through the nozzle, and a higher nozzle temperature leads to a more open structure. It is therefore easier to deform and polarise which is why the birefringence is higher at constant axial pulling stress for higher nozzle temperatures. It was noted by the authors that their results indicated that glass fibres consist of two "portions" – an isotropic one due to thermal history and quenching of the melt (as discussed Section 2.6.2), and an anisotropic portion in the fibre longitudinal direction due to the drawing stress. Birefringence of E-glass fibres has been confirmed by other researchers [52–54].
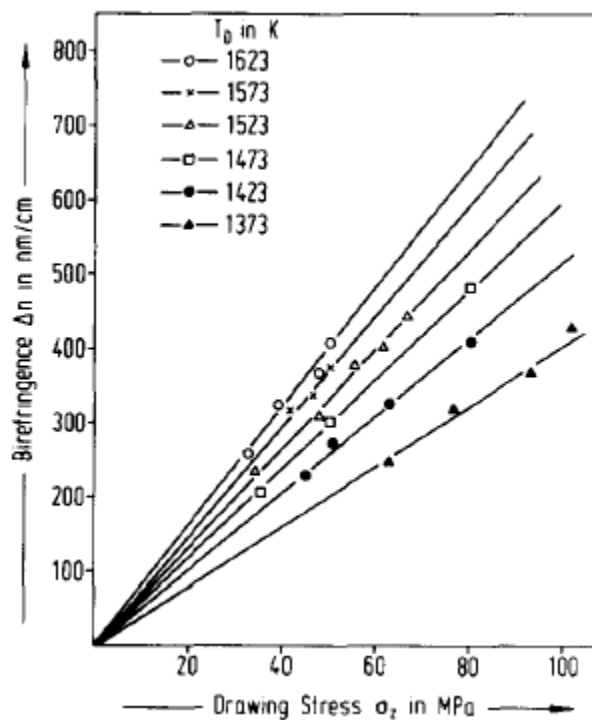

Figure 1: Birefringence of E-glass fibre as a function of the drawing stress; parameter, nozzle temperature [41]

A link between strength and anisotropy of E-glass fibre was investigated [52] using bare fibres that were formed using a range of drawing stress. The strengths of continuous fibres were shown to be higher than those of both the bulk glass and (E-glass) spun wool fibres, whose axial drawing stress was estimated to be around 1 MPa. However, continuous E-glass fibres drawn with stress between 10 – 70 MPa showed no significant difference in their average tensile strengths all of which were in the range 2.5 – 3 GPa.

3. Strength of glass fibre

3.1 Types of strength

The theoretical maximum strength of glass falls somewhere in the range 10 – 30 GPa [55] yet the measured strengths of bulk glasses seldom exceed 50 MPa. Tensile strengths of glass fibres sit somewhere between these extremes with values between 1 – 5 GPa depending on the glass formulation [11]. The strength of E-glass is often quoted as between 2.5 – 4 GPa [8, 11, 13, 56, 57] although in reality the strength of commercially produced fibre, particularly chopped fibres, can be significantly lower. In the context of a given fibre composition such as E-glass there is a maximum intrinsic strength that is measureable; for E-glass this is reported as approximately 6 GPa [56]. To achieve values above even 3 GPa, however, involves a meticulous approach to minimise contact between fibres and any other surfaces. The intrinsic strength is controlled by flaws, as for all glasses, but they are intrinsic to the material.

Extrinsic strength, on the other hand, is controlled by the presence and severity of induced flaws whose size surpasses those of the intrinsic flaws already present. When discussing extrinsic strength this general term 'flaws' may refer to numerous features such as surface scratches and cracks, devitrified regions or unintended inclusions in the bulk material. It is this type of strength that is of interest in practical applications, for example in relation to the strength of HT and recycled glass fibre discussed herein.

3.2 Flaw theory and flaw visualisation

In the discussion of extrinsic strength of glass fibre, flaws are the features of key importance – specifically cracks. A theoretical crack is a 2-dimensional flaw across whose boundary the atomic bonds of the material are broken. Around this flaw stress will be concentrated at the crack tip, which is assumed to be infinitely sharp but in reality must have atomistic dimensions. Cracks are considered the most important type of flaw as only they can grow

under the application of tensile stress [56]. The issue with the infinitely sharp crack tip is that when considering a highly brittle material like glass (where no crack tip blunting occurs) any externally applied stress immediately translates to an infinitely concentrated stress at the tip. The seminal work of Griffith [14] addressed this mathematical issue by considering the problem using an energy balance approach. By application to the case of a uni-axially stressed plate with an edge crack Griffith derived the following equation (1).

$$\sigma_f = \sqrt{\frac{2E\gamma}{\pi a}} \tag{1}$$

In (1) σ_f is the failure stress of the material, E its Young's modulus, γ the surface energy and a is the length of the crack. Although relatively simple, (1) can be acceptably used to describe the behaviour of glass due to its highly brittle nature. In materials with greater ductility a proportion of the released strain energy is dissipated around the crack tip due to plastic flow in the material. A further mathematical modification to (1) comes in the form of the Griffith-Orowan-Irwin Equation (2).

$$a = Y^2 \frac{E\gamma}{\sigma^2} \tag{2}$$

In the form presented, equation (2) may be used to calculate the dimension 'a' of some surface or volume flaw with circular or elliptical shape. Proper use of the equation, however, demands knowledge of the general dimensions of this flaw by some method (such as observation) so that the correct value of the geometric constant Y is chosen. Some values of parameter Y may be obtained in ASTM C1322-05b [58].

Due to their dimensions of the order of only microns in diameter, visualisation of the fracture surfaces of glass fibres is challenging but has been achieved using Scanning Electron Microscopy (SEM). Lund and Yue [59] attempted to systematically correlate strength levels of fibres with flaw types by fractographic analysis of single fibre fracture surfaces but found that there is often no visible flaw at the origin of failure. Even more problematic, a confirmed flaw or crack, critical or otherwise, has never been visualised in an un-fractured glass fibre. An exception to this is the artificial cracks produced in E-glass fibres using Focused Ion Beam (FIB) milling in [60].

4. The effect of elevated temperature on E-glass fibre: changes in strength and to physical and chemical structure

Numerous changes to glass fibres following either direct heat treatment or composite recycling at elevated temperature have been reported in the literature. A decrease in fibre tensile strength is found in almost all cases. In addition, various changes to what can generally be termed the fibre bulk and fibre surface have been described by researchers. Despite the phenomenon being well established the precise mechanism or mechanisms contributing to strength loss from thermal effects remain unclear, as are possible links between known bulk and surface changes and tensile strength loss.

4.1 Strength loss of heat treated glass fibre

Following the discussion in Section 3, a decrease in strength after heat treatment implies that a new and more severe flaw on the GF surface is present compared to the non-heat treated case. This could be a newly formed flaw or have developed from a pre-existing flaw which has grown in size or been made more severe in some other way. Finally, it is possible that some other changes to the GF surface and/or bulk that occur as a consequence of elevated temperature may contribute to failure at a lower stress.

4.1.1 Temperature and time effects

The earliest investigations into strength loss of heat treated E-glass were carried out over 55 years ago [8, 57, 61–63] and established many of the phenomena that remain relevant today. Both Thomas [8] and Cameron [57, 62, 63] showed that retained tensile strength decreases with increasing HT temperature, for all temperatures investigated up to 600 °C. Further work suggested that strength loss proceeds with length of furnace soak time until a constant minimum value is reached, but at higher conditioning temperatures this minimum value is reached within a very short time. These experiments were conducted with lab-produced pristine E-glass without any surface coating, referred to as sizing. In practice it is necessary to apply a tailored sizing to production GF in order to, amongst other things, protect the fibre surface and promote bonding with matrix materials [64, 65]. The findings regarding fibre strength loss have been replicated by Feih et al. using sized E-glass [7, 66]: the trends in strength loss with coupled temperature and time are remarkably similar to those produced by Thomas. Contemporary data regarding strength loss of E-glass using fibres

without sizing are relatively uncommon although some have been produced by Jenkins [5] (shown in Figure 2) et al. and Lund and Yue [52]. The latter of these is somewhat at odds with other data, suggesting that a temperature in excess of 300 °C was necessary to initiate strength loss despite a 3 hour HT. However, this work is of particular interest because measurements of changes in both enthalpy and anisotropy relaxation were made in addition to strength loss. These results are discussed in detail in 4.2.1 and 4.2.2.
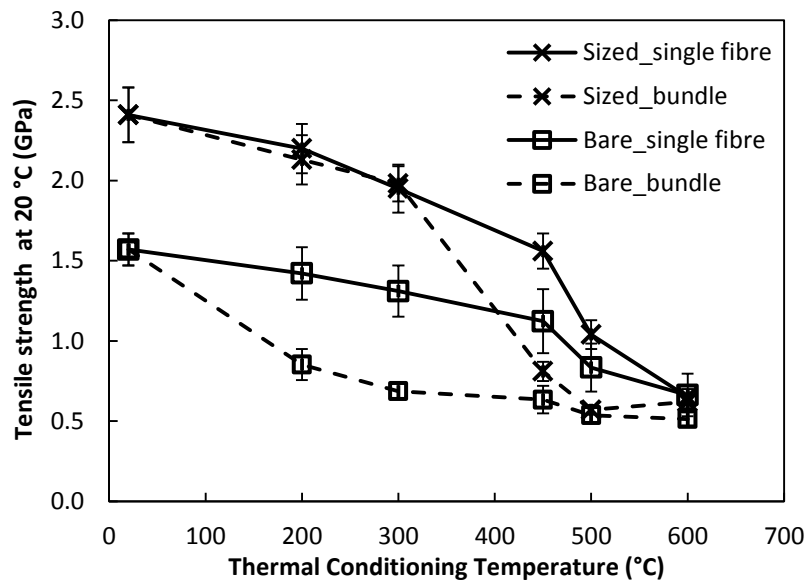

Figure 2: Tensile strengths of bare and Aminopropyltriethoxysilane coated fibre after 25 minute HT [5]

4.1.2 Temperature and mechanical damage

In addition to the effect of elevated temperature alone, mechanical damage inflicted on the surface of GFs can also cause a decrease in strength. In HT and recycling processes both are likely to act simultaneously. It has been demonstrated that by purposefully experimentally minimising the effect of mechanical damage, leaving only thermal effects, the retained strength of HT GF can be significantly increased, by as much as 90 % under some conditions [5]; nonetheless a decrease compared to the untreated fibre strength is found. The effect of fibre mechanical damage during recycling processes can be even more dominant. Kennerley et al. [9] showed tentative results for single glass fibres recovered from both heat-cleaned cloth and composites processed in their Fluidized Bed Combustion (FBC) rig. Although some of the average values reported were based on far smaller sample sizes than preferable for brittle glass, the inverse relationship between retained strength and temperature was observed. Crucially, in this work fibres were exposed to elevated temperatures for short times (20 minutes or less) yet significant strength loss was still measured. In the case of fibres that were FBC processed at 650 °C only 5% of the measured original strength remained.

4.1.3 The effect of heating atmosphere

The effect of the atmosphere in which fibre HT was conducted was a considered variable in work by Cameron [57, 62, 63]. He determined that changes in atmosphere did not produce a significant effect on retained strength, a conclusion verified by the findings of Lund and Yue [52] who treated unsized fibre in either air or nitrogen. Tentative evidence from Feih et al. [7] suggests that an inert atmosphere may retard strength loss of sized fibre for short durations of HT and that this is likely to be related to slowing of the thermal degradation of the sizing. Very little research has been carried out to investigate the possible role of surface water on fibres during HT. Initial results from Jenkins et al. [67], using a simultaneous vacuum and HT process, suggested that there was not a significant change in retained fibre strength for a treatment performed at 450 °C and that water in the atmosphere and on the fibre surface may not, therefore, play a role in strength loss due to HT.

4.1.4 The effect of heat treatment under tensile stress

A rarely investigated phenomenon with respect to the HT of GFs is the effect of applied tensile stress during heating. Despite relatively little attention in the literature the effect produced is of some interest in terms of understanding the strength loss of HT GFs and the mechanism or mechanisms that may be responsible.

Bartenev and Motorina [68] published some early results on fine GFs (diameter approximately 20 µm) of alkaline composition. Initially weak fibres (approximately 1 GPa) presented a linear decrease in strength with HT temperature when heated in stress-free state but an improvement in strength retention was found when a load was applied. Loads equalling 2 or 70 % of the ultimate strength were applied: the former produced a moderate improvement in retained fibre strength after HT, but the latter up to an 100 % increase in comparison with stress-free HT. Cameron [57] made similar findings using E-glass. In this case the fibres had much greater initial strength in excess of 3.5 GPa. The application of a pre-stress of between 2 – 20 % of the room temperature strength led to an improvement in retained strength after HT, although a decrease with respect to the initial value was found. In the discussion of results of these pieces of work the retarded weakening, or strengthening, effect was attributed to alterations to the geometry around cracks or flaws on the fibre surface. Bartenev and Motorina discussed elastic and plastic deformation, and Cameron 'inelastic flow', of material in the vicinity of cracks. In both cases they assumed that this stress-forced flow led to a less critical crack geometry and hence reduced stress concentrations developed when tensile testing was conducted.

Recent investigation of this phenomenon has been carried out by Lezzi et al. [69, 70] using both silica and E-glass, although the fibres used in these works had diameters of approximately 100 μm, greater than mechanical reinforcement GFs by a factor of 5 or more. Despite significant differences in materials their findings were similar to previous investigations. Their explanation for the superior strength retention of fibres was the formation of a thin residual compressive stress layer on the surface of fibres when they are heated under stress while exposed to water vapour; this was confirmed by data gathered using FT-IR and fibre slicing [71].

4.2 Physical and chemical changes following heat treatment

A number of changes to GFs, and E-glass in particular, following HT have been reported which can generally be described as physical or chemical in nature. These are summarised and their potential relevance to GF strength loss is discussed.

4.2.1 Thermal compaction or enthalpy relaxation

A significant bulk phenomenon occurring in E-glass fibre during heating is thermal compaction, first described by Otto and Preston [49] and later investigated in greater detail by Otto [72]. From heating experiments carried out above 300 °C for sufficiently long times a densification process of fine GFs was evidenced by a contraction in their lengths. Similarly, Otto indirectly showed that this process was associated with an increase in Young's modulus. The work of Aslanova et al. [73] demonstrated that the same phenomenon also applied to glass fibre of other compositions. Results showing contraction of fibres in both the longitudinal and radial directions have also been reported [41]. Recently, Otto's findings were verified by Yang and Thomason [74] including direct measurement of the increase in Young's modulus after HT (Figure 3). This agrees with the understanding of the relationship between fictive temperature and Young's modulus presented by Lonnroth et al. [42]. HT below T_g produces a similar effect as that of a slower quenching rate; fictive temperature decreases therefore modulus increases.
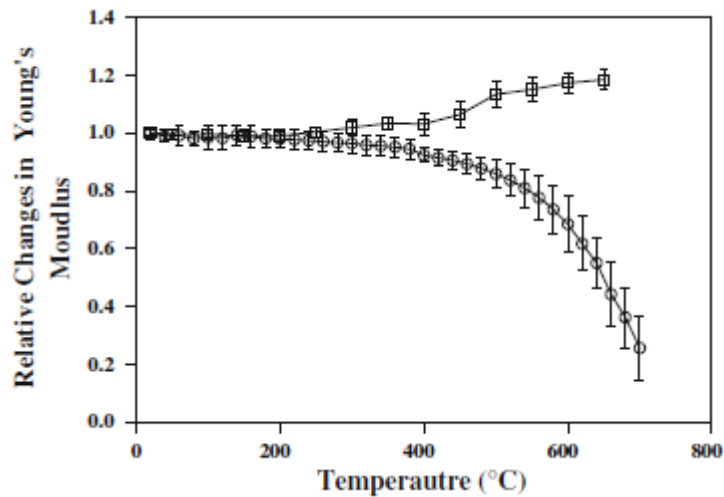
Figure 3: Relative changes in Young's modulus of GFs as a function of temperature (circles) and at room temperature after HT (squares) [74]

Other more recent studies have analysed the relaxation of GFs using Differential Scanning Calorimetry (DSC) [52, 53, 75–77]. They demonstrate that heating below T_g allows the release of what the authors term excess enthalpy from the fibres. The phenomenon is thus called enthalpy relaxation. It was demonstrated [76] that the enthalpy relaxation is related to the quenching of the glass during its production; a larger amount of energy (excess enthalpy) is stored within the glass structure when quenching is performed at a higher cooling rate. The explanation offered for this phenomenon is a "cooperative rearrangement of the frozen-in isotropic network". With respect to E-glass, this rearrangement occurs only once the heat treatment temperature surpasses around 300 ℃ and its rate increases significantly at higher temperatures.

The temperature range over which enthalpy relaxation occurs agrees with that for which fibre length contraction and corresponding increase in Young's modulus occur. It seems reasonable to conclude that these works demonstrate the same phenomenon and that enthalpy relaxation is associated with a long-range relaxation or reorganisation of the glass network producing a denser glass structure. Although this is the case, an explanation of exactly what is happening within the fibre structure during the process has yet to be reported.

A link between thermal compaction/enthalpy relaxation of fibres and the decrease in fibre tensile strength of heat treated fibre is also absent and has yet to be directly investigated. However, an interesting correlation may be noted in the work of Lund and Yue [52]. Using laboratory-produced E-glass fibres they reported that significant strength loss did not occur until HT temperature in excess of 300 ℃ was used, the same temperature at which enthalpy relaxation began.

4.2.2 Anisotropy (birefringence) relaxation

The presence of axial anisotropy in fibres is a function of the drawing parameters and was discussed in 2.6.3. In many studies that report birefringence measurements of GFs experiments were also conducted to analyse the effect of heat treatment [41, 52–54]. Lu et al. [54] suggested that anisotropy relaxation was temperature dependent; complete relaxation occurred if samples were heated to the glass transition temperature (T_g) but lower temperature annealing led to incomplete relaxation. This work was furthered in studies using E-glass fibre [52, 53]. The anisotropy relaxation index, $\Delta n/\Delta n_{max}$, was introduced to describe the remaining fibre anisotropy, where $\Delta n/\Delta n_{max} = 1$ means no relaxation has occurred. Depending on fibre drawing temperature significant reduction in $\Delta n/\Delta n_{max}$ was achieved at HT temperatures between 200 – 300 °C and full relaxation was achieved at temperatures as low as 400 °C given sufficient length of HT.

Similar to enthalpy relaxation, no evidence of a link between anisotropy relaxation and fibre strength loss following HT has been presented but an interesting correlation is noted from the work of Lund and Yue [52]. The same E-glass formulation was used to produce both standard drawn fibres and a spun wool fibre (SWF), the production of which is described in [43]: without fully detailing the SWF production process it is important to note that it is less controlled than fibre drawing, which could allow greater fibre surface damage to occur . These E-glass SWFs produced with minimal axial stress, and hence very low anisotropy, had a measured tensile strength of approximately 1.5 GPa. The anisotropy of continuous E-glass fibres was found to decay to approaching zero after treating at 500 °C for 3 hours; this treatment also caused a decrease in strength from around 3 to 1.5 GPa. From this correlation one could postulate, neglecting additional damage from SWF production, a link between strength loss and anisotropy relaxation.

4.2.3 Crystallisation

Crystallisation of GF due to heat treatment has been proposed as a source of strength loss from work using non-alkaline fibres [78] but these findings have not been reproduced since. There is evidence of nano-crystallisation at the surface of HT basaltic fibres [79] but the mechanism responsible is not applicable to E-glass due to its much lower content of ferric ions. The E-glass formulation is tailored to, in part, eliminate any crystallisation during forming [11] however potential crystallisation of E-glass, for example at the nano scale on the surface, due to HT remains unexplored.

4.2.4 Physical and chemical surface changes

In addition to the phenomena described which represent changes to the bulk structure of E-glass due to heat treatment, some surface phenomena have been reported. In their chemical surface analysis using XPS Nichols et al. observed a Ca depleted surface in comparison to the bulk of E-glass fibres. After heat treating samples for 3 hours at temperatures up to 720 °C it was found that the surface concentration of Ca increased, suggesting that a diffusion process may occur during HT. The strength of GFs after HT was not investigated in this work and no study of the relationship between it and Ca concentration is found in the literature. In general it can be considered unlikely as a mechanism to reduce fibre strength: if an increase in Ca concentration at the glass surface has any effect it appears to correlate with an increase in fracture toughness or strength [80].

Surface roughness of GFs, usually shortly after fibre drawing, have been reported by numerous researchers [81–83]. However, no rigorous studies of change in surface roughness following annealing or HT have been presented in the literature and neither has there been any investigation of any possible link between nano-level surface state and fibre strength, despite the accepted model that failure initiates at the surface unless a significant internal pore has been introduced as a manufacturing flaw.

5. Summary

Temperature induced strength loss of E-glass fibres is a long established phenomenon [8, 57] and, as a brittle material, the fracture mechanics which govern its failure are well understood [14]. Surface flaws with greater severity, due to an increase in dimension or change in geometry, must be present after heat treatment (HT). In some cases mechanical sources of damage may explain the strength loss at least in part [9]; however, a fundamental strength loss caused only by exposure to elevated temperature also exists [5]. It is not well understood by what mechanism this reduction in fibre strength is caused. Interactions between water and the GF surface have at times been postulated although experimental results in this area suggest this may not provide a sufficient explanation [67]. It is known that significant long-range relaxation or reorganisation of the glass network occurs at elevated temperature [52, 53, 72, 74, 77] but no link between this phenomenon and strength loss has been demonstrated. Similarly, relaxation of the anisotropy caused by drawing stresses has been shown from birefringence measurements [41, 52–54] but it is not proven if this is a factor in thermal based strength loss following HT. The efficacy of applied tensile stress during HT to reduce strength loss has been proved and a probable mechanism described [69–71]; however the absence of this mechanism during stress-free fibre HT or recycling

processes does not help to explain the thermal based strength loss that does occur. Further study of the phenomenon is required: initial research into regeneration of the strength of GFs following HT or recycling using surface treatment methods has demonstrated positive results [10, 84], but an improved understanding of the mechanism(s) behind strength loss should help to inform further research in this field.

References

1. Li H, Watson JC (2016) Continuous Glass Fibers for Reinforcement. Encycl. Glas. Sci. Technol. Hist. Cult.

2. Job S (2013) Recycling glass fibre reinforced composites – history and progress. Reinf Plast 57:19–23. doi: 10.1016/S0034-3617(13)70151-6

3. Oliveux G, Dandy LO, Leeke GA (2015) Current Status of Recycling of Fibre Reinforced Polymers: review of technologies, reuse and resulting properties. Prog Mater Sci 72:61–99. doi: 10.1016/j.pmatsci.2015.01.004

4. Pickering SJ (2006) Recycling technologies for thermoset composite materials—current status. Compos Part A Appl Sci Manuf 37:1206–1215. doi: 10.1016/j.compositesa.2005.05.030

5. Jenkins PG, Yang L, Liggat JJ, Thomason JL (2015) Investigation of the strength loss of glass fibre after thermal conditioning. J Mater Sci 50:1050–1057. doi: 10.1007/s10853-014-8661-x

6. Thomason JL, Yang L, Meier R (2014) The properties of glass fibres after conditioning at composite recycling temperatures. Compos Part A Appl Sci Manuf 61:201–208. doi: 10.1016/j.compositesa.2014.03.001

7. Feih S, Boiocchi E, Mathys Z, et al. (2011) Mechanical properties of thermally-treated and recycled glass fibres. Compos Part B Eng 42:350–358. doi: 10.1016/j.compositesb.2010.12.020

8. Thomas WF (1960) An investigation of the factors likely to affect the strength and properties of glass fibres. Phys Chem Glas 1:4–18.

9. Kennerley JR, Fenwick NJ, Pickering SJ, Rudd CD (1997) The properties of glass fibers recycled from the thermal processing of scrap thermoset composites. J Vinyl

Addit Technol 3:58–63. doi: 10.1002/vnl.10166

10. Yang L, Sáez ER, Nagel U, Thomason JL (2015) Can thermally degraded glass fibre be regenerated for closed-loop recycling of thermosetting composites? Compos Part A Appl Sci Manuf 72:167–174. doi: 10.1016/j.compositesa.2015.01.030

11. Wallenberger FT (2010) Commercial and Experimental Glass Fibers. In: Wallenberger FT, Bingham PA (eds) Fiberglass Glas. Technol. Springer US, Boston, MA, pp 3–91

12. Thomason JL, Adzima LJ (2001) Sizing up the interphase : an insider's guide to the science of sizing. Compos Part A Appl Sci Manuf 32:313–321.

13. Wallenberger FT, Watson JC, Hong L (2001) Glass Fibers. In: ASM Handbook, Vol. 21 Compos. ASM International, pp 1–8

14. Griffith AA (1921) The Phenomena of Rupture and Flow in Solids. Philos Trans R Soc A Math Phys Eng Sci 221:163–198. doi: 10.1098/rsta.1921.0006

15. Hair ML (1975) Hydroxyl groups on silica surface. J Non Cryst Solids 19:299–309.

16. Fry R a, Tsomaia N, Pantano CG, Mueller KT (2003) 19F MAS NMR quantification of accessible hydroxyl sites on fiberglass surfaces. J Am Chem Soc 125:2378–2379. doi: 10.1021/ja0275717

17. McDonald RS (1958) Surface Functionality of Amorphous Silica by Infrared Spectroscopy. J Phys Chem 62:1168–1178.

18. Peng L, Qisui W, Xi L, Chaocan Z (2009) Investigation of the states of water and OH groups on the surface of silica. Colloids Surfaces A Physicochem Eng Asp 334:112–115. doi: 10.1016/j.colsurfa.2008.10.028

19. Bakaev VA, Pantano CG (2009) Inverse Reaction Chromatography. 2. Hydrogen/Deuterium Exchange with Silanol Groups on the Surface of Fumed Silica. J Phys Chem C 113:13894–13898.

20. Zhuravlev LT (1993) Surface characterization of amorphous silica - a review of work from the former USSR. Colloids Surfaces A Physicochem Eng Asp 74:71–90.

21. Wesson SP, Jen JS, Nishioka GM (1992) Acid-base characteristics of silane- treated E glass fiber surfaces. J Adhes Sci Technol 6:151–169.

22. Carré A, Lacarrière V, Birch W (2003) Molecular interactions between DNA and an aminated glass substrate. J Colloid Interface Sci 260:49–55. doi: 10.1016/S0021-

9797(02)00147-9

23. Liu XM, Thomason JL, Jones FR (2009) The Concentration of Hydroxyl Groups on Glass Surfaces and their Effect on the Structure of Silane Deposits. In: Mittal KL (ed) Proc. Sixth Int. Symp. Silanes Other Coupling Agents. Brill Academic Publishers, Cincinatti, pp 25–38

24. Pantano CG (2003) Effect of boron oxide on surface hydroxyl coverage of aluminoborosilicate glass fibres: a (19)F solid state NMR study. Phys Chem Glas 44:64–68.

25. Wong R (1972) Recent aspects of Glass Fiber-Resin Interfaces. J Adhes 4:171–179.

26. Thomason JL, Dwight DW (1999) The use of XPS for characterisation of glass fibre coatings. Compos Part A Appl Sci Manuf 30:1401–1413.

27. Nichols D, Hercules DM, Peek RC, Vaughan DJ (1974) Application of X-ray Photoelectron Spectroscopy to the Study of Fiberglass Surfaces. Appl Spectrosc 28:219–222.

28. Wang D, Jones FR, Denison P (1992) TOF SIMS and XPS study of the interaction of hydrolysed γ-aminopropyltriethoxysilane with E-glass surfaces. J Adhes Sci Technol 6:79–98. doi: 10.1163/156856192X00070

29. Fowkes FM, Dwight DW, Cole DA, Huang TC (1990) Acid-Base Properties of Glass Surfaces. J Non Cryst Solids 120:47–60.

30. Martin DM, Akinc M, Oh SM (1978) Effect of Forming and Aging Atmospheres on E-Glass Strength. J Am Ceram Soc 61:308–311.

31. Orowan E (1948) Fracture and strength of solids. Reports Prog Phys 12:185–232. doi: 10.1088/0034-4885/12/1/309

32. Michalske TA, Freiman SW (1982) A molecular interpretation of stress corrosion in silica. Nature 295:511–512.

33. Michalske TA, Freiman SW (1983) A Molecular Mechanism for Stress Corrosion in Vitreous Silica. J Am Ceram Soc 66:284–288.

34. Ito S, Tomozawa M (1982) Crack Blunting of High-Silica Glass. J Am Ceram Soc 65:368–371. doi: 10.1111/j.1151-2916.1982.tb10486.x

35. Nogami M, Tomozawa M (1984) Effect of Stress on Water Diffusion in Silica Glass. J

Am Ceram Soc 67:151–154. doi: 10.1111/j.1151-2916.1984.tb09634.x

36. Tomozawa M (1998) Stress corrosion reaction of silica glass and water. Phys Chem Glas 39:65–69.

37. Tomozawa M, Kim D-L, Agarwal A, Davis KM (2001) Water diffusion and surface structural relaxation of silica glasses. J Non Cryst Solids 288:73–80. doi: 10.1016/S0022-3093(01)00648-2

38. Akinc M, Martin DM (1983) Heat of adsorption of water on E glass fibre surfaces. Phys Chem Glas 24:117–121.

39. Carman LA, Pantano CG (1990) Water-Vapor Adsorption on Calcium-Boroaluminosilicate Glass Fibers. J Non Cryst Solids 120:40–46.

40. Nishioka GM, Schramke JA (1983) Desorption of water from glass fibers. In: Ishida H, Kumar G (eds) Mol. Charact. Compos. Interfaces. Plenum Press, pp 387–400

41. Stockhorst H, Brückner R (1982) Structure sensitive measurements on E-glass fibers. J Non Cryst Solids 49:471–484.

42. Lonnroth N, Muhlstein CL, Pantano CG, Yue Y (2008) Nanoindentation of glass wool fibers. J Non Cryst Solids 354:3887–3895. doi: 10.1016/j.jnoncrysol.2008.04.014

43. Lund MD (2010) Tensile Strength of Glass Fibres. Aalborg University

44. Stockhorst H, Brückner R (1986) Structure sensitive measurements on phosphate glass fibers. J Non Cryst Solids 85:105–126.

45. Brannan RT (1953) Further Evidence Against the Orientation of Structure in Glass Fibers. J Am Ceram Soc 36:230–231.

46. Goldstein M, Davies TH (1955) Glass Fibers with Oriented Chain Molecules. J Am Ceram Soc 38:1953–1956.

47. Miller PJ, Exarhos GJ, Risen WMJ (1973) Vibrational spectral study of molecular orientation in vitreous fibers. J Chem Phys 59:2796. doi: 10.1063/1.1680411

48. Bartenev GM (1969) The Structure and Strength of Glass Fibers of Different Chemical Composition. Mater Sci Eng 4:22–28.

49. Otto WH, Preston FW (1950) Evidence Against Oriented Structure in Glass Fibres. J Soc Glas Technol 34:63–68.

50. Kroenke WJ (1966) Mechanical Test for Anisotropy; Failure of Aluminoborosilicate Glass Fibers Under Combined Loadings of Tension and Torsion. J Am Ceram Soc 49:508–513.

51. Mueller H (1938) Theory of photoelasticity in amorphous solids. J Am Ceram Soc 21:27–33. doi: 10.1111/j.1151-2916.1938.tb15726.x

52. Lund MD, Yue Y (2010) Impact of Drawing Stress on the Tensile Strength of Oxide Glass Fibers. J Am Ceram Soc 93:3236–3243. doi: 10.1111/j.1551-2916.2010.03879.x

53. Ya M, Deubener J, Yue Y (2008) Enthalpy and Anisotropy Relaxation of Glass Fibers. J Am Ceram Soc 91:745–752. doi: 10.1111/j.1551-2916.2007.02100.x

54. Lu X, Arruda E., Schultz W. (1999) The effect of processing parameters on glass fiber birefringence development and relaxation. J Nonnewton Fluid Mech 86:89–104. doi: 10.1016/S0377-0257(98)00203-1

55. Sugarman B (1967) Strength of Glass (A Review). J Mater Sci 2:275–283.

56. Gupta PK (2002) Strength of Glass Fibers. In: Elices M, Llorca J (eds) Fiber Fract. Elsevier Ltd, pp 125–153

57. Cameron NM (1968) The effect of environment and temperature on the strength of E-glass fibres. Part 2. Heating and ageing. Glas Technol 9:121–130.

58. ASTM C1322-05b (2010) Standard Practice for Fractography and Characterization of Fracture Origins in Advanced Ceramics. doi: 10.1520/C1322-05BR10.2

59. Lund MD, Yue Y (2008) Fractography and tensile strength of glass wool fibres. J Ceram Soc Japan 116:841–845. doi: 10.2109/jcersj2.116.841

60. Feih S, Mouritz AP, Case SW (2015) Determining the mechanism controlling glass fibre strength loss during thermal recycling of waste composites. Compos Part A Appl Sci Manuf 76:255–261. doi: 10.1016/j.compositesa.2015.06.006

61. Sakka S (1957) Effect of Reheating on Strength of Glass Fibers. Bull Inst Chem Res 34:316–320.

62. Cameron NM (1962) The Effect of Annealing on the Room Temperature Strength of Glass Fibres. Illinois

63. Cameron NM (1965) Effect of Prior Heat Treatment on the Strength of Glass Fibers

Measured at Room Temperature. J Am Ceram Soc 48:385.

64. Thomason JL (2012) Glass Fibre Sizings, 1st ed.

65. Mäder E, Jacobasch H-J, Grundke K, Gietzelt T (1996) Influence of an optimized interphase on the properties of polypropylene/glass fibre composites. Compos Part A Appl Sci Manuf 27:907–912. doi: 10.1016/1359-835X(96)00044-9

66. Feih S, Manatpon K, Mathys Z, et al. (2008) Strength degradation of glass fibers at high temperatures. J Mater Sci 44:392–400. doi: 10.1007/s10853-008-3140-x

67. Jenkins PG, Riopedre-Mendez S, Sáez Rodríguez E, et al. (2015) Investigation of the strength of thermally conditioned E-glass and basalt fibres (presentation). 20th Int. Conf. Compos. Mater.

68. Bartenev GM, Motorina LI (1965) Effect of Tensile Stresses on the Strength of Heat-Treated Glass Fibers. Mekhanika Polim [Translated] 1:89–92.

69. Lezzi PJ, Xiao QR, Tomozawa M, et al. (2013) Strength increase of silica glass fibers by surface stress relaxation: A new mechanical strengthening method. J Non Cryst Solids 379:95–106. doi: 10.1016/j.jnoncrysol.2013.07.033

70. Lezzi PJ, Seaman JH, Tomozawa M (2014) Strengthening of E-glass fibers by surface stress relaxation. J Non Cryst Solids 402:116–127. doi: 10.1016/j.jnoncrysol.2014.05.029

71. Lezzi PJ, Tomozawa M (2015) An Overview of the Strengthening of Glass Fibers by Surface Stress Relaxation. Int J Appl Glas Sci 1–11. doi: 10.1111/ijag.12108

72. Otto WH (1961) Compaction Effects in Glass Fibers. J Am Ceram Soc 44:68–72.

73. Aslanova MS, Ivanov N V, Balashov YS (1970) Effect of chemical composition on the relaxation properties of thin glass fibers. Steklo i Keramika 8:21–24.

74. Yang L, Thomason JL (2013) The thermal behaviour of glass fibre investigated by thermomechanical analysis. J Mater Sci 48:5768–5775. doi: 10.1007/s10853-013-7369-7

75. Yue Y, Jensen SL, Christiansen J de C (2002) Physical aging in a hyperquenched glass. Appl Phys Lett 81:2983. doi: 10.1063/1.1514386

76. Yue Y (2005) Features of the relaxation in hyperquenched inorganic glasses during annealing. Phys Chem Glas 46:354–358.

77. Deubener J, Yue Y, Bornhöft H, Ya M (2008) Decoupling between birefringence decay, enthalpy relaxation and viscous flow in calcium boroalumosilicate glasses. Chem Geol 256:299–305. doi: 10.1016/j.chemgeo.2008.06.052

78. Aslanova MS (1960) The Effect of Different Factors on the Mechanical Properties of Glass Fibers. Steklo i Keramika 17:10–15.

79. Yue Y, Korsgaard M, Kirkegaard LF, Heide G (2009) Formation of a Nanocrystalline Layer on the Surface of Stone Wool Fibers. J Am Ceram Soc 92:62–67. doi: 10.1111/j.1551-2916.2008.02801.x

80. Dériano S, Jarry A, Rouxel T, et al. (2004) The indentation fracture toughness (Kc) and its parameters: The case of silica-rich glasses. J Non Cryst Solids 344:44–50. doi: 10.1016/j.jnonerysol.2004.07.021

81. Rondinella V V., Matthewson MJ, Kurkjian CR (1994) Coating Additives for Improved Mechanical Reliability of Optical Fiber. J Am Ceram Soc 77:73–80. doi: 10.1111/j.1151-2916.1994.tb06959.x

82. Gupta PK, Inniss D, Kurkjian CR, Zhong Q (2000) Nanoscale roughness of oxide glass surfaces. J Non Cryst Solids 262:200–206. doi: 10.1016/S0022-3093(99)00662-6

83. Mellott NP, Pantano CG (2013) A Mechanism of Corrosion-Induced Roughening of Glass Surfaces. Int J Appl Glas Sci 4:274–279. doi: 10.1111/ijag.12035

84. Thomason JL, Nagel U, Yang L, Sáez ER (2015) Regenerating the strength of thermally recycled glass fibres using hot sodium hydroxide (submitted). Compos Part A Appl Sci Manuf. doi: 10.1017/CBO9781107415324.004